JBC RESEARCH ARTICLE

RKIP localizes to the nucleus through a bipartite nuclear localization signal and interaction with importin α to regulate mitotic progression

Received for publication, May 12, 2022, and in revised form, January 13, 2023 Published, Papers in Press, February 15, 2023,
https://doi.org/10.1016/j.jbc.2023.103023

Christian E. Argueta[1], **Christopher Figy**[2], **Sawssen Bouali**[3], **Anna Guo**[2], **Kam C. Yeung**[2], **and Gabriel Fenteany**[3,4,*]

From the [1]*Department of Chemistry, University of Connecticut, Storrs, Connecticut, USA;* [2]*Department of Cell and Cancer Biology, University of Toledo College of Medicine, Toledo, Ohio, USA;* [3]*Department of Medical Chemistry, University of Szeged, Szeged, Hungary;* [4]*ELKH-SZTE Biomimetic Systems Research Group, Eötvös Loránd Research Network, Szeged, Hungary*

Reviewed by members of the JBC Editorial Board. Edited by Donita Brady

Raf kinase inhibitor protein (RKIP) is a multifunctional modulator of intracellular signal transduction. Although most of its functions have been considered cytosolic, we show here that the localization of RKIP is primarily nuclear in both growing and quiescent Madin-Darby canine kidney epithelial cells and in Cal-51 and BT-20 human breast cancer cells. We have identified a putative bipartite nuclear localization signal (NLS) in RKIP that maps to the surface of the protein surrounding a known regulatory region. Like classical NLS sequences, the putative NLS of RKIP is rich in arginine and lysine residues. Deletion of and point mutations in the putative NLS lead to decreased nuclear localization. Point mutation of all the basic residues in the putative NLS of RKIP particularly strongly reduces nuclear localization. We found consistent results in reexpression experiments with wildtype or mutant RKIP in RKIP-silenced cells. A fusion construct of the putative NLS of RKIP alone to a heterologous reporter protein leads to nuclear localization of the fusion protein, demonstrating that this sequence alone is sufficient for import into the nucleus. We found that RKIP interacts with the nuclear transport factor importin α in BT-20 and MDA-MB-231 human breast cancer cells, suggesting importin-mediated active nuclear translocation. Taken together, these findings suggest that a bipartite NLS in RKIP interacts with importin α for active transport of RKIP into the nucleus and that this process may be involved in the regulation of mitotic progression. Evaluating the biological function of nuclear localization of RKIP, we found that the presence of the putative NLS is important for the role of RKIP in mitotic checkpoint regulation in MCF-7 human breast cancer cells.

Raf kinase inhibitor protein (RKIP) belongs to a highly conserved group of proteins in the phosphatidylethanolamine-binding protein (PEBP) family and possesses a plethora of functions (for reviews, see Refs. (1–9)). The most widely expressed member of this family is RKIP or PEBP-1 (10, 11). RKIP, as its name implies, inhibits the activity of Raf-1 kinase (12, 13). RKIP also binds and regulates the function of G protein-coupled receptor kinase 2 (GRK2); the phosphorylation of a specific residue on RKIP (Ser 153) catalyzed by PKC causes RKIP to dissociate from Raf and instead associate with GRK2, and the phosphorylation of Ser 153 is a key part of the regulation of the functions of RKIP (14, 15). RKIP has been shown to bind a number of other proteins as well, including B-Raf (16, 17), extracellular signal-regulated kinase (ERK) (13), mitogen-activated protein kinase (MAPK)/ERK kinase (12, 13), transforming growth factor β-activated kinases 1 (18), NF-κB-inducing kinase (NIK) (18), inhibitor of κB kinase α (IKKα) and β (IKKβ) (18), and tumor necrosis factor receptor–associated factor 6 (19). RKIP or PEBP-1, as its latter name implies, also binds to phosphatidylethanolamine (20) and may be involved in membrane signaling (21); however, the interaction with phosphatidylethanolamine is weak and appears nonspecific (22).

RKIP has been implicated in a range of biological processes, such as the regulation of cell cycle progression (23–26), apoptosis (27, 28), cell migration (22, 26, 28–33), cell adhesion (32), neural function (34–36), cardiac function (37), and spermatogenesis (38). Intriguingly, there is ever-growing evidence that RKIP functions as a suppressor of invasion and metastasis in a range of cancer cell types (for reviews, see Refs. (1–9)). Despite its modest size (∼21 kDa), a protein with functions that are as multifaceted as RKIPs would likely have a complex pattern of regulation for appropriate expression, post-translational modification, interaction, and localization.

Despite RKIP being an intracellular protein, a fragment of RKIP does appear to be secreted as the hippocampal cholinergic neurostimulating peptide (37). RKIP has been traditionally thought of as a protein that functions in the cytosol, without consideration of possible nuclear functions. Small proteins can passively diffuse in and out of the nucleus (for a review, see Ref. (39)). RKIP is small enough to potentially pass through nuclear pores passively, implying that some mechanism operates to control the localization of RKIP such as association with other proteins to form complexes too large to passively enter or exit the nucleus. RKIP interacts with a growing number of proteins in a post-translationally regulated

* For correspondence: Gabriel Fenteany, fenteany.gabriel@med.u-szeged.hu.
Present address for Christian E. Argueta: Takeda Pharmaceuticals, Cambridge, Massachusetts, USA.

manner. These regulated interactions could control the localization of RKIP in the cell.

Active nuclear translocation is necessary to regulate specific cellular functions such as control of gene expression, DNA replication, cell division, and cell differentiation (for a review, see Ref. (40)). Proteins that require tight regulation of nuclear localization generally contain clusters of basic residues—arginines and lysines—called nuclear localization signals (NLSs) (for reviews, see Refs. (41, 42)). These signals can occur as individual clusters or as two or three clusters separated by varying numbers of amino acid residues (usually 10–12). When more than one cluster appears, they are referred to as bipartite or tripartite NLSs. The basic residues of a classical NLS bind to transport proteins known as importins or karyopherins, of which there are two major families, the importin α proteins and the importin β proteins (for review, see Refs. (43, 44). Generally, importin α isoforms recognize various classical NLS types and then bind importin βs (45). The importin α/β heterodimer then associates with the nuclear pore complex, allowing for entry of the NLS-containing protein into the nucleus. Once inside the nucleus, the GTP-bound Ran protein binds importin β, and its cargo is released (46). Some NLSs contain a phosphorylatable residue near the signal that usually interferes with complex formation but, in other cases, phosphorylation increases the affinity of the cargo protein for importin α (for a review, see Ref. (47)), including the SV40 T antigen (48) and the Hsp70/Hsp90-organizing protein (49).

We report here that RKIP localizes primarily to the nucleus in Madin-Darby canine kidney (MDCK) epithelial cells, both in cultures that are subconfluent (with growing cells) and those that are confluent (with quiescent cells). We also found similar results in Cal-51 triple-negative human breast cancer cells, as well as in RKIP reexpression experiments in RKIP-silenced BT-20 human triple-negative breast cancer cells. We confirmed by confocal microscopy that RKIP localizes inside the nucleus (nucleoplasm) in MDCK cells. We identified a putative classical bipartite NLS consisting of 146-RGKFKVASFRKK-157 toward the C terminus of the protein by bioinformatics analysis. We confirmed that the putative NLS sequence mediates nuclear transport of RKIP by analyzing the localization of RKIP point mutants of the putative NLS and an RKIP deletion mutant fused to GFP or GFP along with glutathione-*S*-transferase (GST). The regulatory serine residue 153, whose phosphorylation state helps determine which binding partner RKIP associates with, is located within this putative NLS sequence. We also found that the mutation of certain basic residues (substitution of arginines and lysines with asparagines alone and in combination) within the sequence impairs the nuclear accumulation of RKIP, consistent with the functioning of the sequence as an NLS. Fusion of the putative NLS sequence to GFP led to a greater nuclear accumulation of GFP when compared with GFP alone. RKIP interacts with an importin α isoform(s) in both BT-20 and MDA-MB-231 human triple-negative breast cancer cells. The putative NLS in RKIP is important to the function of RKIP in mitotic checkpoint control during the cell cycle in MCF-7 human breast cancer cells.

Results

RKIP localization in the nucleus

MDCK cells immunofluorescently stained with an antiRKIP antibody were examined for localization of RKIP, and nuclei were visualized by staining with the DNA-binding fluorescent dye 4′,6-diamidino-2-phenylindole (DAPI). RKIP was localized mainly to the nucleus (Fig. 1*A*). Immunofluorescent staining with an anti-phospho-RKIP (Ser 153) antibody also showed marked nuclear localization, as well as localization along the edges of cells (Fig. 1*B*). Images obtained from slides in which MDCK cells were subconfluent (Fig. 1, *A* and *B*), so still growing, and also confluent (Fig. 1, *C–E*), so quiescent, revealed nuclear localization for both total RKIP and phospho-RKIP. Confocal microscopy of cells stained immunofluorescently for total RKIP and visualized in an intranuclear *z*-plane slice revealed that RKIP is predominately distributed within the nucleoplasm and not in a perinuclear fashion (Fig. 1*E*).

Evaluating other cell types, we found that the strong nuclear localization of RKIP is not unique to MDCK cells. Endogenous RKIP also primarily localized to nuclei in Cal-51 cells (Fig. 2), as did reexpressed wildtype RKIP in RKIP-depleted BT-20 cells (Fig. 6, see additional results with these cells later), as revealed by confocal immunofluorescence microcopy after staining with an anti-RKIP antibody.

Bioinformatic identification of a putative NLS in RKIP

We analyzed the full-length sequence of human RKIP with the PredictNLS program (50) and identified a possible classical bipartite NLS stretching from amino acids 146 to 157. The sequence consists of two clusters of basic residues with a glycine in the sequence, which tends to prevent the formation of any traditional secondary structure. The sequence contains the Ser 153 that has been shown to undergo regulatory phosphorylation by PKCα and PKCδ (14, 15). We also queried the NetNES 1.1 (51) and LocNES (52) programs, which search for classical leucine-rich nuclear export signals, with the full human RKIP sequence and did not find any high-scoring hits (the latter did predict with very low confidence a possible nuclear export localization signal at residue positions 23–37).

Mapping the putative NLS onto the three-dimensional RKIP structure

The putative NLS is highlighted in Figure 3 on a human RKIP X-ray crystal structure with Protein Data Bank (PDB) accession code 1BD9 (21). The putative NLS is on the surface and solvent exposed, which would allow for access by importin α. The small linker sequence folds inward, bringing both basic clusters together, as is the case in other similar NLSs. The sequence also maps to the same location on the surface of other mammalian RKIP structures (PDB codes: 1A44, 1BEH, 1B7A, 2IQY, 2QYQ, and 2IQX) (21, 53–55), as well to the

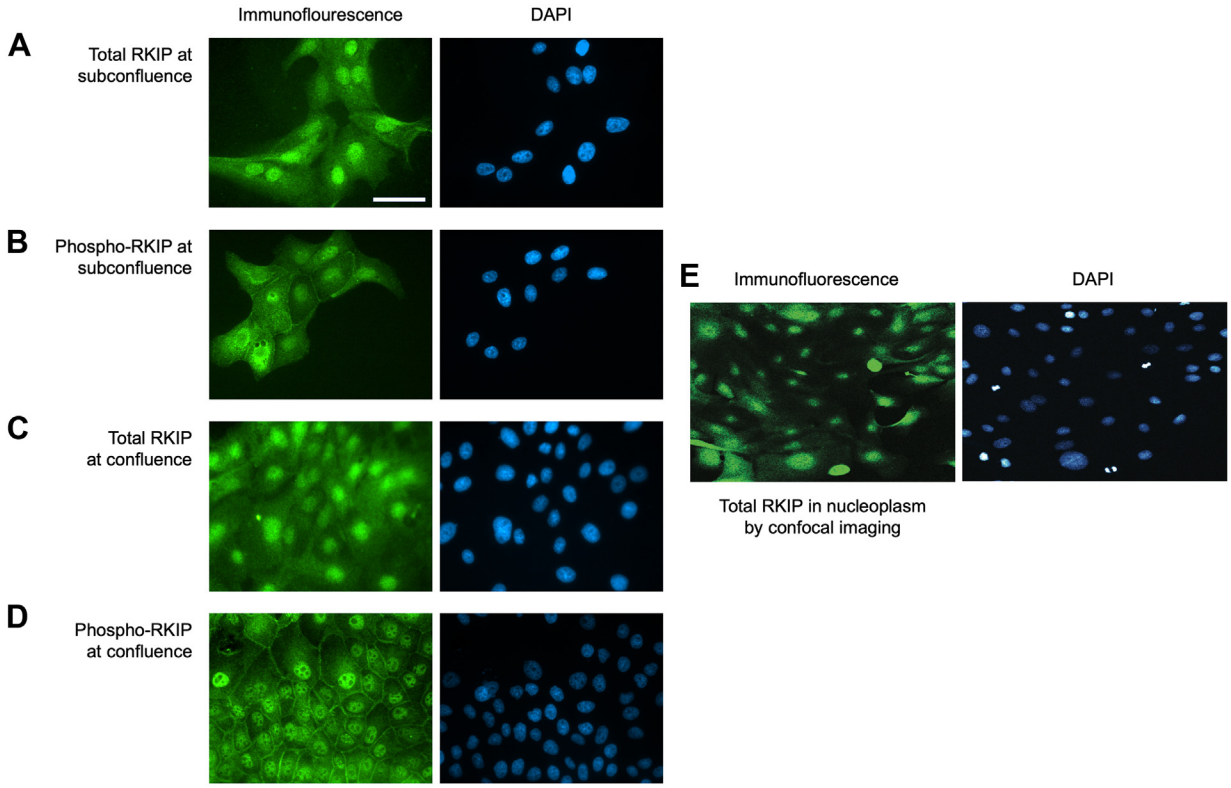

Figure 1. Endogenous RKIP localizes to the nucleus of epithelial cells. *A*, cellular localization of total RKIP (RKIP and phospho-RKIP) in MDCK canine kidney epithelial cells at subconfluent cell density so that the cells are still growing. *B*, cellular localization of endogenous phospho-RKIP (Ser 153) in MDCK cells at subconfluent cell density such that cells are still proliferating. *C*, cellular localization of endogenous RKIP in MDCK cells at confluent cell density such that the cells are quiescent. *D*, cellular localization of endogenous phospho-RKIP in MDCK cells at confluent cell density. *E*, confocal image of the cellular localization of endogenous total RKIP (RKIP/phospho-RKIP) taken in an intranuclear plane, demonstrating nucleoplasmic rather than perinuclear localization. The cells were fixed with formaldehyde, permeabilized, and probed with either an anti-pan-RKIP antibody that recognizes both unphosphorylated and phosphorylated RKIP or an anti-phospho-RKIP (Ser 153)- antibody, and localization was visualized with Alexa Fluor 488-conjugated secondary antibody. Nuclei were visualized with the DNA stain DAPI. The scale bar in the *first panel* on the *left* represents 50 μm, with all images at the same magnification. All images are representative of at least three independent experiments.

corresponding region of the murine PEBP-2 structure (PDB code: 1KN3) (56), but is not found in bacterial, protozoan, or plant homologs of RKIP/PEBP. The human sequence is identical to that in the bovine protein and almost identical to the rat protein (where Ala 151 is instead a Glu residue).

GFP-GST-fused RKIP with a C-terminal deletion localizes exclusively to the cytoplasm

We investigated whether RKIP is localized to the nucleus through an active transport mechanism, despite its small size, and confirmed that the sequence predicted by the PredictNLS program (50) is necessary for nuclear localization. We generated two "large" chimeric proteins that are less likely to passively diffuse across nuclear pores. GFP was fused to full-length GST-RKIP (amino acids 1–187) and a GST-RKIP deletion mutant (amino acids 1–134), with the putative NLS missing. The GST fusions have been previously described by Yeung *et al.* (13). The full-length GFP-GST-RKIP fusion protein (~72 kDa) was still able to enter the nucleus in MDCK cells, whereas the smaller GFP-GST-RKIP deletion mutant (~67 kDa) composed of amino acid residues 1 to 134, lacking the putative NLS, displayed reduced nuclear localization (Fig. 4).

GFP fused to RKIP with mutated putative NLS sequences results in decreased nuclear localization

To explore whether this sequence was indeed involved in nuclear localization, we created various point mutations: six single mutants, two triple mutants, and one hexamutant with every basic residue mutated in the putative NLS (Table 1) The arginine and lysine residues were replaced by asparagine residues instead of the oft-used alanine to conserve the hydrophilic nature of the residues. The wildtype and mutant versions of RKIP were fused to GFP to visualize them in the cell. After generating stable transfectants, we observed altered localization in certain point mutants when compared with the control, which corresponds to a ca. 2:1 nuclear:cytoplasmic localization ratio by image analysis (Fig. 5). In addition to the single point mutations, the triple mutants also showed decreased nuclear localization when compared with the control. The most dramatic difference was observed with the 146-**N**G**N**F**N**VASF**NNN**-157 hexamutant (mutated residues indicated in boldface) with a nuclear:cytoplasmic ratio of 0.97, which would correspond to free equilibration between nucleus and cytoplasm, indicating that the sequence indeed promotes nuclear localization (Table 1 and Fig. 5*B*). To further

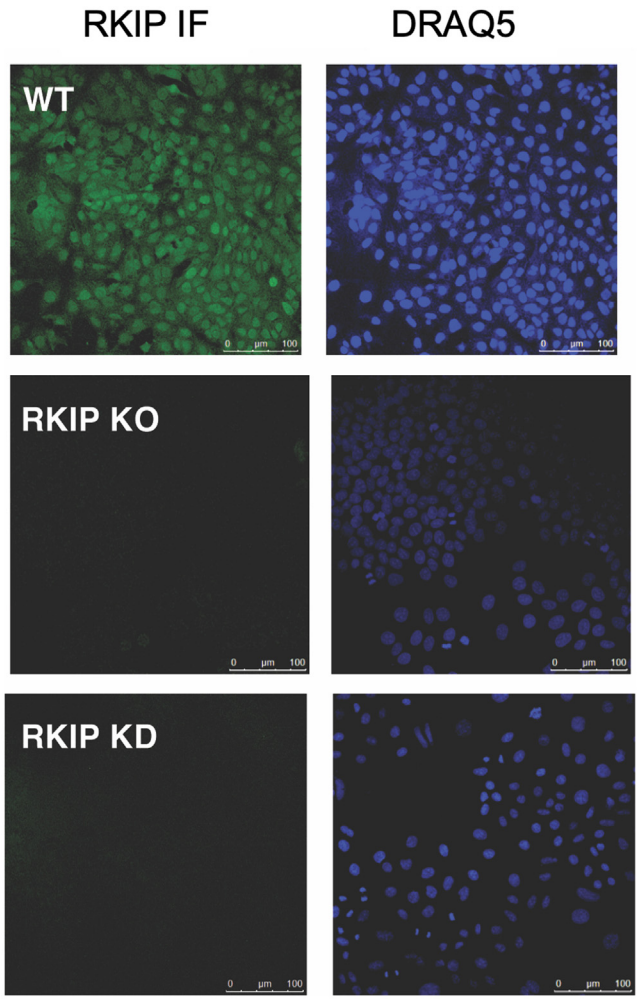

Figure 2. Endogenous RKIP localizes to the nucleus of Cal-51 human triple-negative breast cancer cells. Representative images of immunofluorescent staining with an anti-RKIP antibody and the DNA stain DRAQ5. RKIP knockdown (KD) and RKIP KO Cal-51 cells were used as primary antibody negative controls. IF, immunofluorescence; RKIP, Raf kinase inhibitor protein.

investigate the function of the identified putative NLS, we reexpressed either wildtype or RKIP NLS mutants in BT-20 cells that were previously depleted of RKIP expression by a specific siRNA. Similar to the results for MDCK and Cal-51 cells, RKIP-depleted BT-20 cells restored with wildtype RKIP displayed prominent nuclear localization of RKIP staining. Importantly, the RKIP NLS hexamutant showed lower nuclear localization (Fig. 6).

GFP fused to the putative NLS sequence localizes to the nucleus

We further examined whether the sequence by itself indeed functions as an NLS when fused to a heterologous protein. We fused the NLS sequence to the C terminus of a GFP construct. While GFP appears to be able to passively diffuse through nuclear pores (57), we used a single GFP gene fused to the putative NLS for convenience and looked at accumulation above control levels in the fusion. The GFP-NLS fusion was localized to a significantly greater extent to the nucleus and the plasma membrane than GFP alone (Fig. 7, *A* and *B*).

RKIP interacts with an importin α isoform(s) in cells

To determine whether the nuclear transport of RKIP into the nucleus is likely to occur through an importin-mediated pathway, we performed coimmunoprecipitation experiments with RKIP in FLAG-RKIP-expressing BT-20 cells and found that FLAG-RKIP interacts with endogenous importin α by probing with an anti-importin α5 (karyopherin α1) antibody (Fig. 8*A*). We also looked at interaction of endogenous RKIP to endogenous importin α in MDA-MB-231 cells by probing with an anti-importin α5/α7 (karyopherin α1/α6) antibody, finding that importin α again coimmmunoprecipitated with RKIP (Fig. 8*B*). We obtained similar results in MDCK cells and COS-7 African Green monkey kidney fibroblasts (unpublished data).

The nuclear localization of RKIP is required for its effect on mitotic checkpoint regulation

RKIP has been shown to have a likely function in mitotic checkpoint regulation, with siRNA-mediated depletion of RKIP resulting in decreased numbers of metaphase cells and shortened traversal times from prophase to anaphase (24). We examined whether the putative NLS in RKIP may be involved in this process. Reexpression of wildtype RKIP, but not the RKIP NLS hexamutant, restored the shortened normal traversal time from nuclear envelope breakdown to anaphase resulting from the silencing of RKIP expression in MCF-7 cells (Fig. 9). The effect is not cell line specific as we found that Cal-51 cells exhibited similar changes on mitotic progression upon RKIP knockdown and reexpression of the RKIP NLS hexamutant compared with the reexpression of wildtype RKIP (unpublished results).

Discussion

RKIP is small enough to be able to passively diffuse into the nucleus, but its localization in the nucleus has not been examined before. We report here that the primary localization of RKIP and phospho-RKIP (Ser 153) in MDCK epithelial cells is in the nucleus (Fig. 1, *A* and *B*). We found consistent results in Cal-51 cells (Fig. 2), as well as in reexpression experiments with wildtype and NLS mutant RKIP in RKIP-silenced BT-20 cells (Fig. 6). Similar results for phospho-RKIP have been reported during mitosis prior to nuclear envelope breakdown in HeLa cervical carcinoma cells and Ptk-1 rat kangaroo kidney epithelial cells (24, 25), although in MDCK cells, RKIP appears to localize to the nucleus during interphase as well, as evidenced by images taken from quiescent cells in confluent cell monolayers (Fig. 1, *C* and *D*). Observation of endogenous RKIP and phospho-RKIP confirmed that the protein is located inside the nucleus (Fig. 1). By confocal microscopy of an intranuclear *z*-plane slice, we found that it is localized throughout the nucleoplasm and not confined to a perinuclear or other subnuclear location (Fig. 1*E*). We identified the sequence 146-

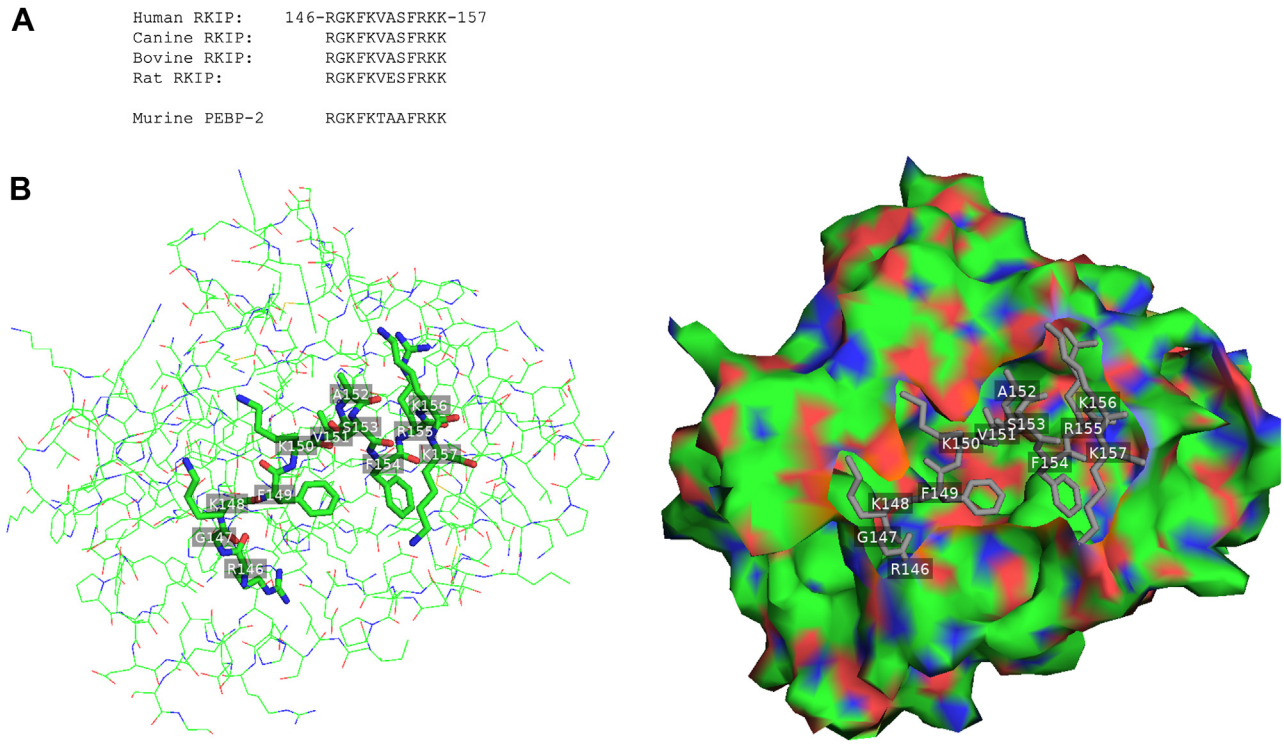

Figure 3. Mapping of the putative nuclear localization signal (NLS) to the surface of RKIP. *A*, Putative mammalian RKIP/PEBP-1 and PEBP-2 NLS sequences, predicted from analysis with the PredictNLS program (50). *B,* Putative NLS highlighted on a human RKIP X-ray crystal structure PDB code: 1BD9 (54) with PyMOL (http://www.pymol.org/) in licorice-stick format for the NLS against wire-line rendition (*left*) and filled-surface rendition (*right*) of the rest of the protein. The highly conserved putative NLS maps to the same location on the surface of other mammalian RKIP structures (PDB codes: 1A44, 1BEH, 1B7A, 2IQY, 2QYQ, and 2IQX) (21, 53–55), as well as in the murine PEBP-2 structure (PDB code: 1KN3) (56), but not in bacterial or protozoan homologs of RKIP/PEBP.

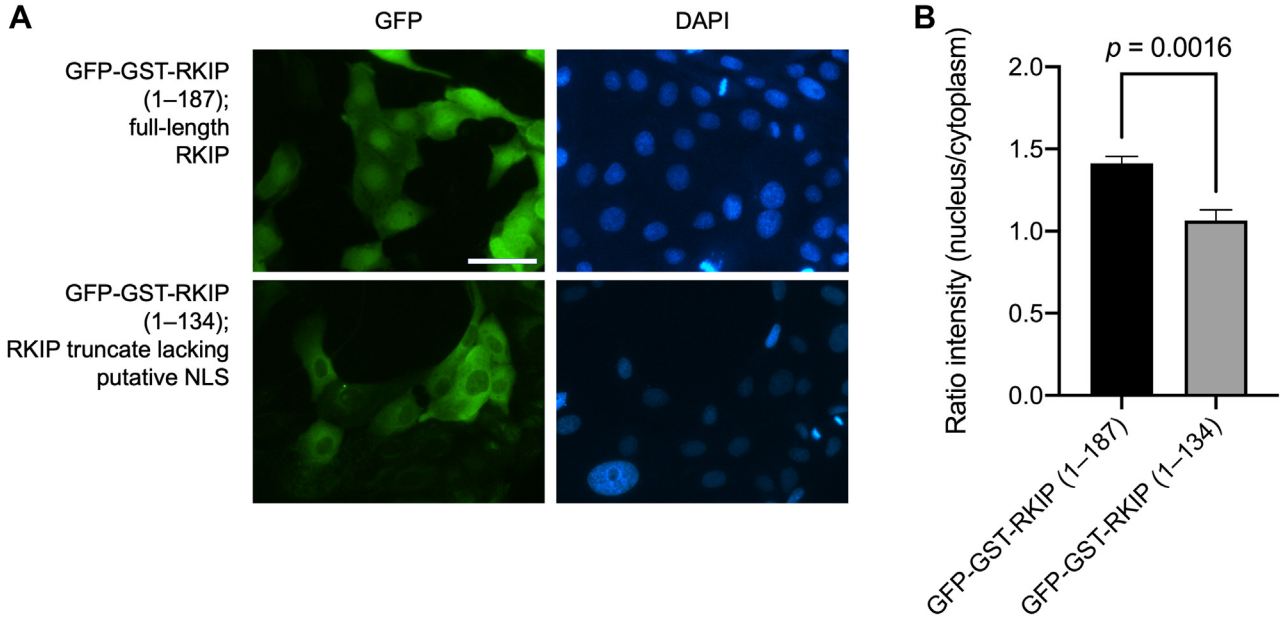

Figure 4. Deletion of the C terminus of RKIP, which contains the putative nuclear localization signal (NLS), abrogates the nuclear localization of RKIP. *A*, cellular localization of full-length wildtype RKIP (amino acids 1–187) and an RKIP truncate (C-terminal deletion mutant consisting only of amino acids 1–134), each fused to GFP-glutathione-*S*-transferase (GST) in Madin–Darby canine kidney (MDCK) cells. Stable transfectants were plated onto glass coverslips and fixed 24 h later. Nuclei were visualized with the DNA stain DAPI and imaged in the same field of view as the images for GFP fluorescence. Representative images from at least three independent experiments are shown in each case. The scale bar in the *first panel* on the *left* represents 50 μm, with all images at the same magnification. *B*, ratio of total nuclear GFP fluorescence to total cytoplasmic GFP fluoresence quantitated from the microscope images of wildtype RKIP fused to GFP-GST or the RKIP truncate (which lacks the putative NLS) fused to GFP-GST. The mean and SEM are shown, with *p* value for difference by unpaired two-tailed Student's *t* test.

Table 1
Point mutants generated in the arginine and lysine residues that define the putative bipartite NLS of RKIP

Sequence	Mutant name
146-RGKFKVASFRKK-157	Wildtype putative NLS
146-NGKFKVASFRKK-157	R146N
146-RGNFKVASFRKK-157	K148N
146-RGKFNVASFRKK-157	K150N
146-RGKFKVASFNKK-157	R155N
146-RGKFKVASFRNK-157	K156N
146-RGKFKVASFRKN-157	K157N
146-NGNFNVASFRKK-157	R146N, K148N, K150N
146-RGKFKVASFNNN-157	R155N, K156N, K157N
146-NGNFNVASFNNN-157	R155N, K148N, K150N, R155N, K156N, K157N (hexamutant)

RGKFKVASFRKK-157 in RKIP, containing two close clusters of basic amino acids, as having a high probability of being a classical bipartite NLS based on analysis with the PredictNLS program (50). Examination of the crystal structure of RKIP showed that the putative NLS is solvent exposed and is thus potentially accessible to importin α proteins (Fig. 3). This relatively C-terminal sequence in RKIP is highly conserved and is present at the surface of all mammalian RKIP/PEBP-1 structures solved and uploaded to the PDB database. The putative NLS is also present at the surface of murine PEBP-2. However, weakly homologous sequences in bacterial and protozoan RKIP/PEBP homologs for which three-dimensional structures are available in the PDB do not map to those proteins' surface, although a partly homologous sequence in the RKIP/PEBP homolog from the plant *Arabidopsis thaliana*, FLOWERING LOCUS T protein, does map to the protein's surface. The location of the putative NLS at the surface of mammalian RKIP/PEBP-1 structures uploaded to the PDB suggests an important and conserved nuclear function for RKIP, at least in mammals.

Shuttling in and out of the nucleus can generally occur passively across the nuclear pore complex of the nuclear envelope for proteins smaller than ∼40 kDa (for a review, see Ref. (58)). A number of small proteins have been reported to be actively translocated into the nucleus. The small GTPase Rac1 (21 kDa) possesses an NLS and is actively transported into the nucleus in a cell cycle–dependent manner (59–61). The 21-kDa protein histone H1° possesses multiple NLS elements, interacts with importin α, and translocates into the nucleus by an active mechanism (62). Galectin-3 (26 kDa) can enter the nucleus both passively and by an importin-mediated NLS-dependent active pathway and is degraded more rapidly in the absence of active nuclear transport (63, 64). The matrix protein of the vesicular stomatitis virus has a size of 27 kDa and contains two different NLS sequences that mediate active transport into the nucleus (65–68). While it is clear that small proteins can have NLS motifs and be actively transported into the nucleus, it is interesting to speculate as to why this is so. First of all, passive diffusion would not allow for unidirectional vectorial translocation into the nucleus and enrichment above a concentration at which the protein would simply equilibrate between nucleus and cytoplasm, unless there were an anchoring or sequestration protein located in the nucleus and passive nuclear exit were thus prevented. Secondly, smaller proteins may associate with other proteins to form larger complexes in the cytoplasm that are too big for passive diffusion but have nuclear functions. In such cases, an NLS on even a small protein in the complex could help mediate active transport of the entire complex from the cytoplasm into the nucleus.

Although RKIP is small enough at 21 kDa to potentially passively diffuse into the nucleus, it is not evenly distributed in the cell and appears to localize predominately in the nucleus. We constructed a larger fusion protein (GFP-GST-RKIP) that was ∼72 kDa to examine whether size was the only factor in RKIP nuclear localization. The fusion protein still exhibited nuclear localization (Fig. 4). On the other hand, a slightly smaller fusion (GFP-GST-RKIP 1–134), with a size of ∼67 kDa and lacking the C terminus with the putative NLS, did not localize to the same degree to the nucleus (Fig. 4). Single point mutations of the basic residues in the GFP-GST-RKIP fusion proteins led to decreased nuclear localization. Although individual mutations only resulted in slightly decreased localization in the nucleus, multiple point mutation of basic residues in the putative NLS led to uniform distribution throughout the cell (Fig. 5).

Conversely, we examined bioinformatically whether a classical nuclear export signal may reside in RKIP and found no solid evidence for the presence of one. Either cytoplasmic movement of RKIP from the nucleus is controlled by a more cryptic nuclear export signal or release from binding partners in the nucleus allows for passive diffusion across nuclear pores back to the cytosol.

Fusing the putative NLS to GFP led to a significantly higher degree of nuclear distribution (Fig. 7, *A* and *B*). The GFP control localized primarily to the nucleus as well but to a lesser extent and with more diffuse distribution when compared with that of the GFP-NLS fusion protein (Fig. 7, *A* and *B*). This, along with the mutation and deletion protein results, show that the C terminus of RKIP is integral to the nuclear localization process and that the sequence 146-RGKFKVASFRKK-157 serves as a *bona fide* NLS. We also found that RKIP interacts with an importin α isoform(s) in cells, through coimmunoprecipitation of stably expressed FLAG-RKIP in BT-20 cells or of endogenous RKIP in MDA-MB-231 cells (Fig. 8, *C* and *D*). Similar results were also obtained in MDCK and COS-7 cells (unpublished data). The collective results strongly suggest that RKIP is actively transported into the nucleus by an importin-mediated pathway.

A number of studies have shown that nuclear import can be upregulated and downregulated by phosphorylation on residues located near an NLS in other proteins (for a review, see Ref. (47)). RKIP contains a conserved serine residue (Ser 153), a known site of RKIP phosphorylation and regulation in other contexts (14, 15), located between the two basic regions of the putative bipartite NLS. It is possible that the nuclear localization and function of RKIP could be regulated by phosphorylated on this residue.

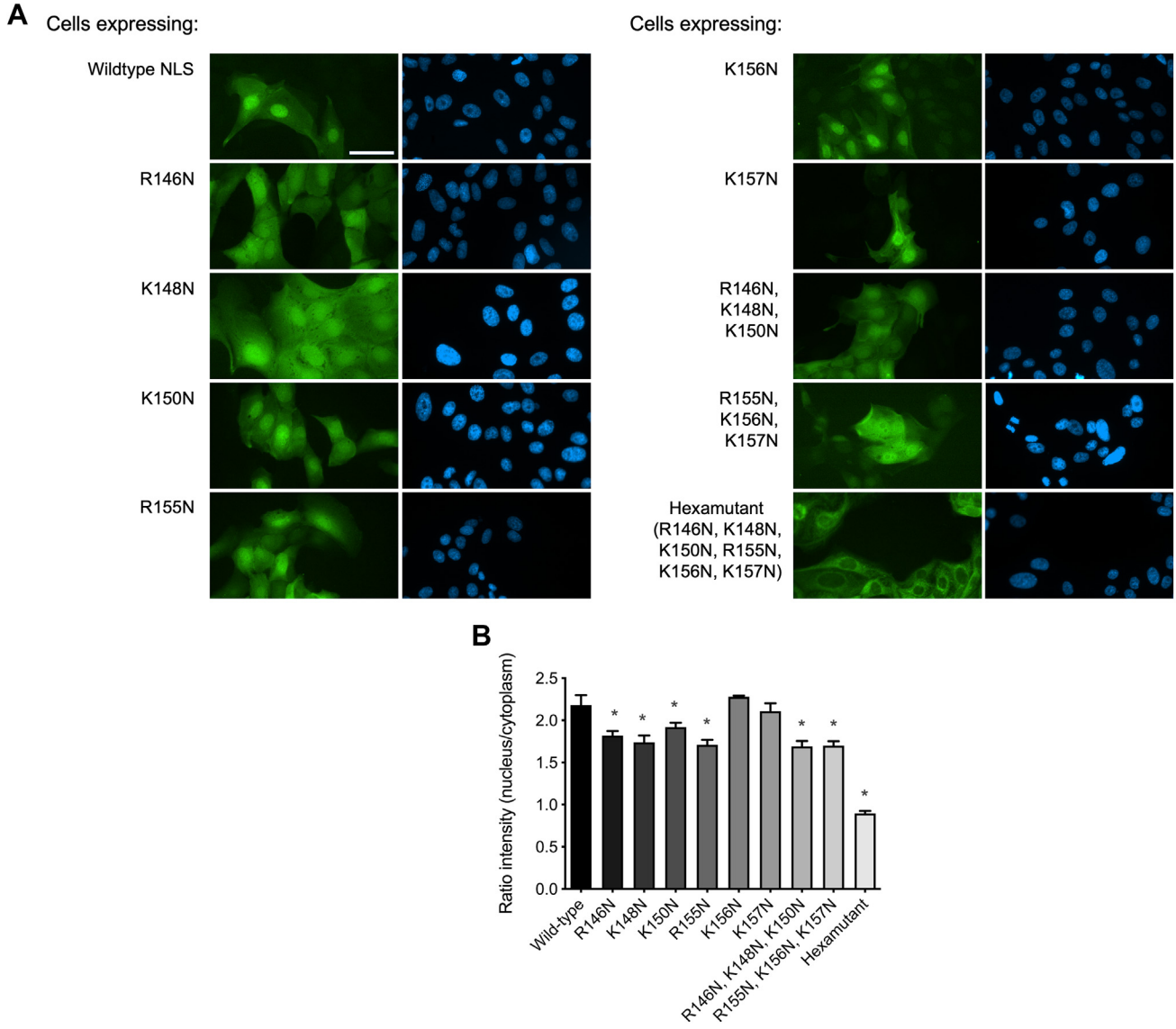

Figure 5. Cellular localization of GFP fused with wildtype RKIP is predominately nuclear, whereas GFP-fused RKIP point mutants in the putative nuclear localization signal (NLS) revealed decreased nuclear localization. *A*, cellular localization of wildtype RKIP and indicated RKIP mutants in the putative NLS fused to GFP expressed in Madin-Darby canine kidney (MDCK) cells is shown. Cells stably expressing GFP fusion proteins were plated onto glass coverslips and fixed 24 h later. Nuclei were visualized by DAPI staining and imaged in the same field of view as the images for GFP fluorescence. Scale bar in the *first panel* on the *left* represents 50 μm, with all images at the same magnification. Images are representative of at least three independent experiments in each case. *B*, the localization of RKIP in over 40 cells was quantified and is represented in the bar graph. The bars show the nuclear:cytoplasmic ratio expressed as the mean with SEM derived from three independent experiments. *Asterisks* indicate significant difference of $p < 0.05$ by individual unpaired two-tailed Student's *t* tests relative to control.

RKIP appears to regulate a mitotic checkpoint(s) in normal and cancer cells (24, 25). Downregulation of RKIP expression relaxes the mitotic checkpoint with subsequent decrease in the number of mitotic cells and shortened metaphase to anaphase transition (24). The putative NLS we have identified appears critical to the function of RKIP in mitotic checkpoint regulation (Fig. 9). Our results raise the possibility that the mitotic function of RKIP requires its presence in the nucleus before the breakdown of the nuclear envelope during mitosis. It is possible that RKIP regulates mitotic progression control by interacting with nuclear mitotic checkpoint regulatory proteins. The importance of the putative NLS in RKIP thus suggests that RKIP needs to be imported into the nucleus prior to nuclear envelope breakdown to fulfill its function in subsequent mitotic checkpoint control.

Enrichment in the nucleus to higher concentrations than achievable through simple passive equilibration across the nuclear envelope may be required for RKIP to fulfill its as-yet unclear nuclear functions. Moreover, since RKIP forms many different larger complexes that may be too big for passive diffusion into the nucleus, the putative NLS of RKIP could allow for transport of both RKIP and its bound interacting partners into the nucleus. RKIP binds myriad proteins including kinases involved in MAPK signaling such as Raf-1 (12, 13), B-Raf (16, 17) (though possibly without significant functional effects), ERK (13), and MAPK/ERK

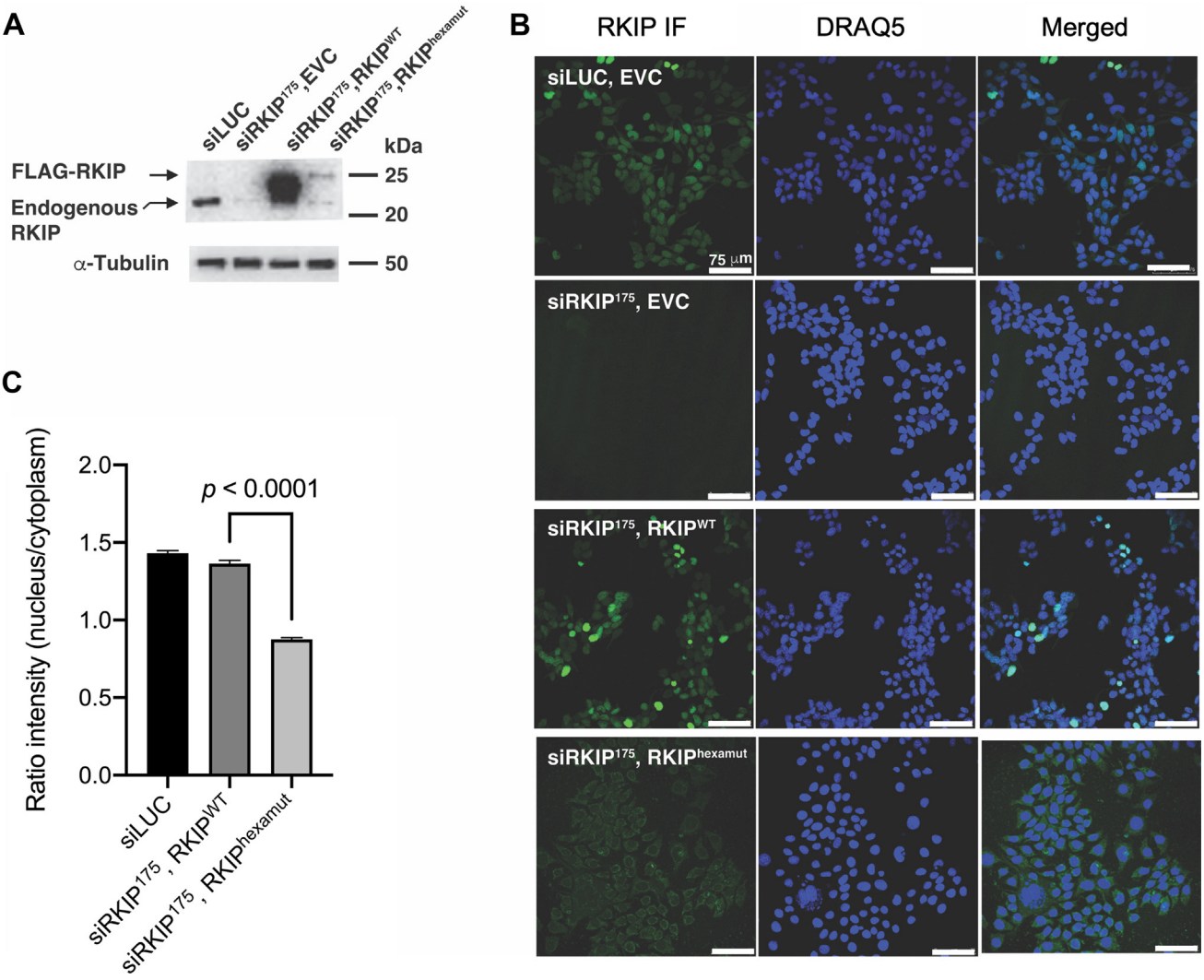

Figure 6. Localization of RKIP also involves the putative nuclear localization signal (NLS) in BT-20 human triple-negative breast cancer cells. *A*, representative Western blot of BT-20 cells stably integrated with different combinations of the indicated constructs: (1) siLUC (control siRNA not affecting RKIP expression) and empty vector control (EVC); (2) RKIP-knockdown (siRNA^{175}) cells and EVC; (3) RKIP-knockdown cells re-expressing wildtype RKIP (RKIP^{WT}); and (4) RKIP-knockdown cells expressing RKIP NLS hexamutant (RKIP^{hexamut}). *B*, cellular localization of RKIP and RKIP NLS hexamutant in BT-20 cells described in *A*, showing nuclear localization of wildtype RKIP and reduced nuclear localization of the RKIP NLS mutant. Cells were fixed with methanol and then incubated with an anti-RKIP antibody for RKIP immunofluorescence (IF) and the DNA stain DRAQ5 for nuclear visualization. *C*, quantitation of RKIP immunofluorescent staining intensity in the cytoplasm and nucleus from the microscope images, expressed as mean and SEM, with *p* value for indicated comparison by unpaired two-tailed Student's *t* test.

kinase (12, 13). RKIP also binds and regulates the function of GRK2 (14, 15) and kinases involved in NF-κB processing (transforming growth factor β-activated kinase 1, NIK, IKKα, IKKβ (18), and tumor necrosis factor receptor–associated factor 6 (19)). Furthermore, RKIP may have scaffolding functions and so form even higher order complexes, at least transiently (19).

In summary, upon noticing nuclear localization of endogenous RKIP in MDCK epithelial cells, an observation that seems to have not been made before, we found a sequence that has high homology to a canonical bipartite NLS, and this sequence appears integral to the nuclear localization of RKIP in MDCK, Cal-51, and BT-20 cells. Furthermore, the presence of the putative NLS is required for RKIP function in mitotic checkpoint regulation in MCF-7 cells as well as in Cal-51 cells. We excluded the possibility of passive diffusion as the only method for nuclear translocation and found that RKIP interacts with importin α. The phosphorylation of the important regulatory serine (Ser 153), which lies in the middle of the putative NLS, could play a role in controlling the nuclear localization of RKIP. Collectively, these data demonstrate the hitherto ignored fact that RKIP is heavily localized to the nucleus, at least in the epithelial and carcinoma cell lines we examined. To our knowledge, no other publication has explicitly reported on the nuclear localization and function of RKIP. The presumption has always been that it operates mainly in the cytoplasm. This makes the present study timely and significant, and it may stimulate new ways of thinking about RKIP and new areas for the further study of this important multifunctional signaling regulatory protein.

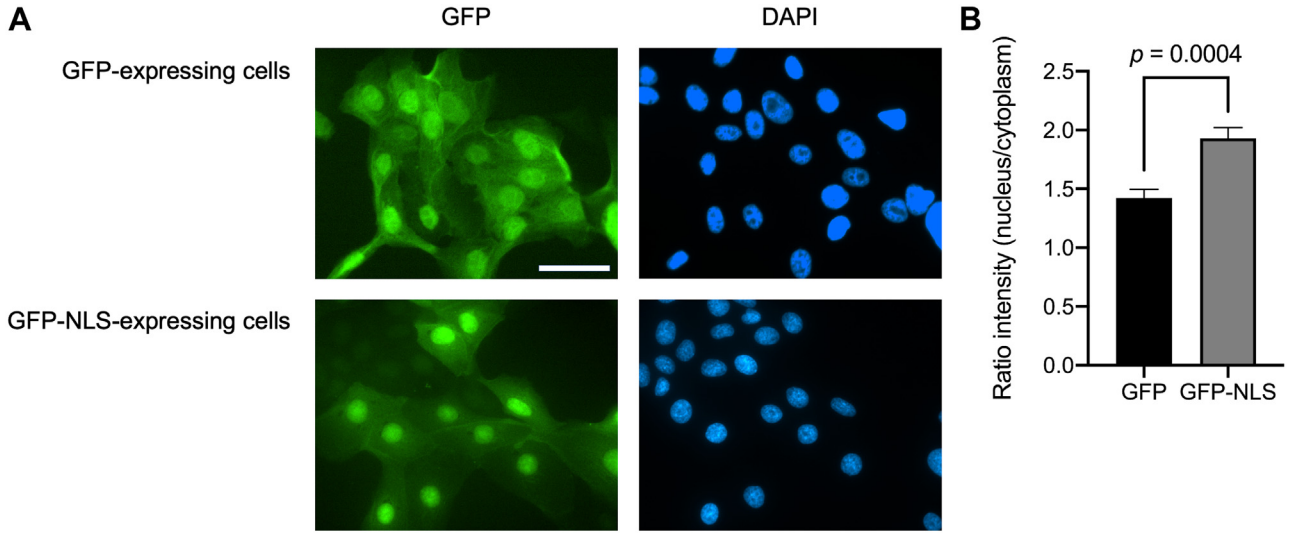

Figure 7. Fusion of RKIP's putative nuclear localization signal (NLS) to GFP alone results in its nuclear localization. *A*, cellular localization of GFP in Madin–Darby canine kidney (MDCK) cells. Cellular localization of the putative NLS of RKIP (amino acid residues: 146-RGKFKVASFRKK-157) fused to the C terminus of GFP alone. Stable transfectants expressing GFP and GFP-NLS were plated onto glass coverslips and fixed 24 h later. Scale bar in the *first panel* on the *left* represents 50 μm, with all images at the same magnification. Images are representative of at least three independent experiments. *B*, nuclear:cytoplasmic ratio of GFP fluorescence from the microscope images of GFP-expressing and GFP-NLS-expressing cells (mean and SEM shown, with *p* value for difference by Student's *t* test).

Experimental procedures

Cell culture

MDCK cells were cultured in minimum essential medium containing 10% newborn calf serum in a humidified incubator at 37 °C with 5% CO_2. Cal-51, BT-20, and MCF-7 histone H2A-red fluorescent protein (H2A-RFP) fusion–expressed cells were cultured in Dulbecco's modified Eagle's medium (HyClone) with 10% fetal bovine serum (HyClone), and 1% penicillin–streptomycin (HyClone). MDCK and BT-20 cells were purchased from American Type Culture Collection. Cal-51 and H2A-RFP-expressing MCF-7 cells were generous gifts from Drs Song-Tao Liu (University of Toledo) and Jason Sheltzer (Cold Spring Harbor Laboratory), respectively.

Construction of GFP-tagged RKIP and RKIP mutants for expression in cells

Human RKIP was cloned into the pEF6-GFP-Myc-His B vector. Point mutant constructs were generated utilizing primers designed with the Agilent QuikChange Primer Design program. GST-tagged rat RKIP wildtype and deletion mutant constructs were amplified from the PGEX-KG vector and cloned into the pEF6-GFP-Myc-His B vector. The NLS

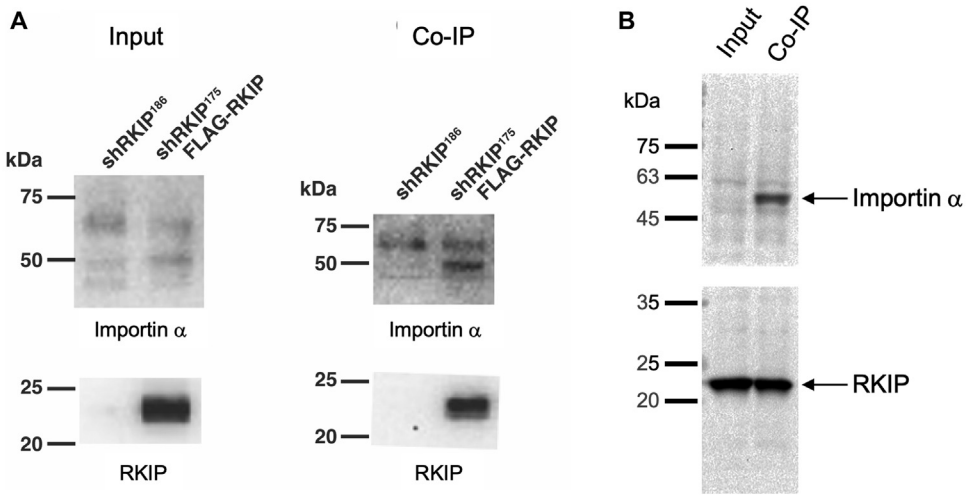

Figure 8. Importin α interacts with RKIP in cells. *A*, RKIP binds importin α in cells. FLAG-RKIP expressed on BT-20 cells interacts with importin α by coimmunoprecipation with an anti-FLAG antibody. Western blot of cell lysate input and coimmunoprecipitated (co-IP) samples, probed with anti-importin α5 (karyopherin α1) antibody and anti-RKIP antibody, is representative of three independent experiments. *B*, endogenous RKIP interacts with endogenous importin α in MDA-MB-231 human triple-negative breast cancer cells by immunoprecipitation with an anti-RKIP antibody. Western blot of cell lysate input and co-IP samples, probed with anti-importin α5/α7 (karyopherin α1/α6) antibody and anti-RKIP antibody, is representative of four independent experiments. We obtained similar results in Madin–Darby canine kidney (MDCK) cells and COS-7 African green monkey kidney fibroblasts (unpublished data).

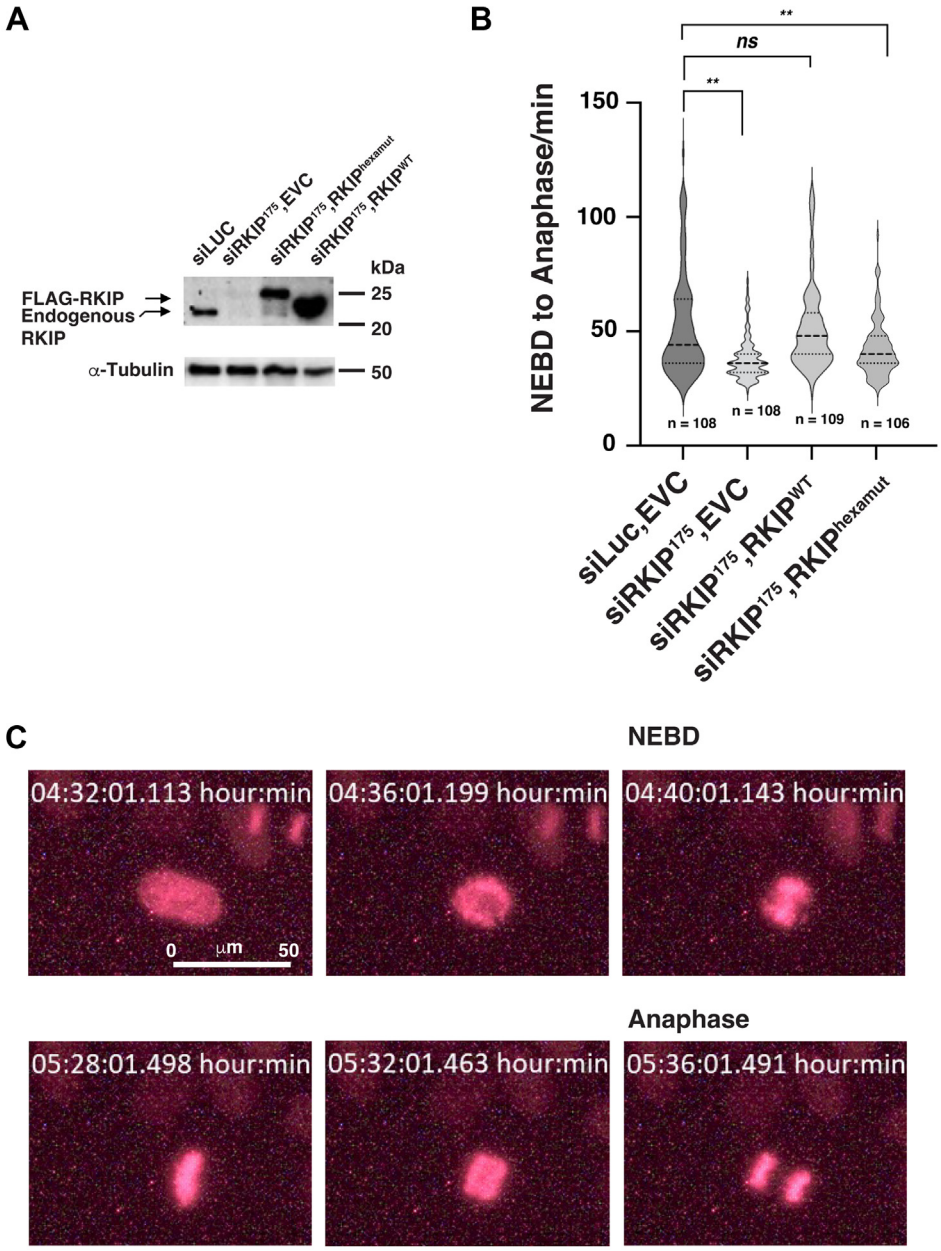

Figure 9. The putative nuclear localization signal (NLS) in RKIP is required for its RKIP's function in mitotic checkpoint control. *A*, Western blot showing expression of endogenous RKIP, FLAG-RKIP, and α-tubulin in MCF-7 human breast cancer cells stably expressing red fluorescent protein (RFP)-tagged histone H2A and the following expression constructs: (1) siLuc as a control expressing an siRNA to firefly luciferase; (2) RKIP knockdown (siRKIP^{175}), complemented with empty vector control (EVC); (3) RKIP knockdown (siRKIP^{175}), complemented with an RKIP NLS hexamutant construct (RKIP^{hexamut}); and (4) RKIP knockdown (siRKIP^{175}), complemented with a wildtype RKIP construct (RKIP^{WT}). *B*, comparison of mitosis duration of indicated MCF-7 expressing different complementary DNA (cDNA) constructs from nuclear envelope breakdown (NEBD) to anaphase onset. ns, not significant; $^{**}p < 0.05$ by unpaired two-tailed Student's *t* test; *n*, number of cells analyzed. In addition to these experiments in MCF-7 cells, we carried out preliminary experiments in Cal-51 cells and obtained similar results on the effect of the RKIP NLS hexamutant in mitotic progression. *C*, representative microscope images of cells over the course of the time-lapse videos, showing progress to NEBD to anaphase.

sequence was generated by PCR amplification and cloned into the pEF6-GFP-Myc-His B vector. The constructs were all sequenced to confirm each point mutation or the deletion. They were then transfected into MDCK cells with Lipofectamine 2000 according to the manufacturer's protocol (Invitrogen). Stable transfectants were selected for 3 weeks with, and subsequently also maintained in, blasticidin S (10 μg/ml). For the experiments involving BT-20 cells and MCF-7 cells, wildtype or mutant RKIP constructs were retrovirally delivered into cells for stable expression.

Fluorescence microscopy

MDCK cells were plated onto 12-mm coverslips, fixed 24 h later with 3.7% formaldehyde in PBS for 20 min, permeabilized with 0.5% Triton X-100 in PBS for 10 min, and then mounted on microscope slides in MOWIOL 4-88 containing 1,4-diazabicyclo[2.2.2]octane. For immunofluorescence, cells were incubated with a rabbit anti-RKIP antibody (Santa Cruz Biotechnology; catalog no.: sc-28837) or a rabbit anti-phospho-RKIP (Ser 153) antibody (Santa Cruz Biotechnology; catalog no.: sc-32622) and stained with goat anti-rabbit

immunoglobulin G (IgG) conjugated to Alexa Fluor 488 (Invitrogen). DAPI was used to stain the nuclei. The slides were observed on a Leica DMI 6000B inverted fluorescence microscope. Images were captured with a Hamamatsu Orca AG cooled charge-coupled device camera.

Nuclear localization of RKIP by confocal microscopy was examined to determine if the localization was throughout the nucleoplasm or perinuclear only. The confocal images were obtained with a Nikon A1R-A1 microscope system with NIS Elements Viewer software.

For the experiments with the Cal-52 cell line, cells were plated on laminin-coated (MilliporeSigma) glass coverslips and grown until a visual confirmed desired confluency is reached. Cells were washed with 1× PBS and fixed with −20 °C 100% methanol for 10 min. Coverslips were incubated overnight with a mouse anti-RKIP antibody (Santa Cruz Biotechnology; RKIP H-10, catalog no.: sc-376925) followed by 1 h incubation with goat anti-mouse IgG conjugated to Alexa Fluor 594 (1:2000 dilution; Thermo Fisher). Nuclei were visualized with the DNA stain DRAQ5 (1:2000 dilution; Cell Signaling Technology) before cells were mounted with PermaFluor (Thermo Fisher). Fluorescence images were captured with a Leica TCS SP5 multiphoton laser scanning confocal microscope.

For quantification of nuclear and cytoplasmic protein localization, three fields of view were imaged at random per slide with three slides for each stably transfected cell line for a total of nine fields of view. For image analysis, nuclei and cytosols of cells were traced to determine the sum of the fluorescence intensity in each traced area. Background intensity was subtracted by tracing an empty area of the image and subtracting that value from the individual nuclear and cytoplasmic fluorescence signals. The values were then expressed as a ratio of signals in the nucleus over the cytoplasm with Prism software (GraphPad Software, Inc).

Time-lapse microscopy

MCF-7 cells expressing the H2A-RFP fusion protein were plated on a 6-well plate in Dulbecco's modified Eagle'-s medium with 10% fetal bovine serum and 1% penicillinstreptomycin (HyClone). Cells were synchronized with 2 mM thymidine (MilliporeSigma) in culture medium for 16 to 18 h under normal incubation conditions (37 °C and 5% CO_2), followed by washing and release into culture medium. The plate was moved to a preincubated live cell imaging chamber associated with the Zeiss Axio Observer 3/5/7 KMAT microscope used for imaging. Cells were incubated (37 °C and 5% CO_2) for 2 h prior to time-lapse image acquisitions. We randomly selected four points in each well containing cells. Each of these positions was imaged at 20× magnification every 4 min over the course of 18 h. Focus was confirmed manually prior to beginning imaging process. Analysis was done with Zeiss Zen 3.4 software.

Nuclear membrane breakdown (NEBD) was determined based on changes in morphology visualized by time-lapse imaging of the fluorescent H2A-RFP fusion protein in the nucleus. Prior to NEBD, the nucleus is generally static and can be described as a smooth bean in shape. When NEBD has occurred, the nuclear edge is no longer smooth, and the DNA begins condensing to the metaphase plate. The distinct change in morphology to the nucleus was marked as frame 1/time 0:00 for the duration analysis. The total number of frames that pass between this observation and full separation of daughter chromatids during late anaphase was counted and multiplied by four to give the duration of this process in minutes, and the duration was confirmed by comparing the time stamps of the two frames of interest. Data were plotted with GraphPad Prism software to visualize the data and determine averages of each group. Unpaired two-tailed Student's *t* tests were performed to compare different groups.

Preparation of RKIP-knockdown, RKIP-knockout, or RKIP-expressing cells

RKIP-knockdown cells were generated with RNA interference–based silencing as previously described (33). CRISPR-Cas9 was used to knockout the RKIP gene in Cal-51 cells by published methods (69). Successful knockdown or knockout were confirmed by Western blot analysis. Retrovirus-mediated gene transfer was used to reexpress wildtype or mutant RKIP in RKIP-knockdown BT-20 cells. Expression of the tagged RKIP fusions was confirmed by Western blot analysis.

Coimmunoprecipitation experiments

Proliferating RKIP knockdown or FLAG-tagged RKIP-rescued knockdown BT-20 cells were harvested and lysed in PBS with 10% glycerol and 0.5% Triton X-100 on ice for 30 min. Samples were clarified by centrifugation at 14,000*g* for 10 min at 4 °C, and the supernatant was collected. Total protein concentration was determined by Bradford assay (70) with Bio-Rad protein assay dye reagent. Clarified cell lysates (500 µl at 1.4 mg/ml protein concentration) were incubated with 50 µl of a 50% slurry of monoclonal anti-FLAG M2 affinity gel (MilliporeSigma). Samples were incubated with gentle agitation for 4 h at 4 °C. After incubation, samples were washed three times with PBS containing 10% glycerol, 0.5% Triton X-100, and 250 mM NaCl. Immunoprecipitated proteins were separated by SDS-PAGE and transferred to 0.45 µm pore polyvinylidene difluoride membranes (Merck Millipore). After transfer, the blots were cut in half by molecular weight. The upper part was probed with rabbit anti-importin α5 (karyopherin α1) antibody (MyBioSource; catalog no.: MBS719156) at 1:1000 dilution overnight at 4 °C in PBS with 0.2% Tween-20, 3% bovine serum albumin, and 0.02% sodium azide. The lower part was probed with rabbit anti-RKIP antibody (12) at 1:1000 dilution for 1 h at room temperature. The membranes were subsequently incubated with goat anti-rabbit IgG-horseradish peroxidase secondary antibody (MilliporeSigma). Proteins were visualized by chemiluminescence.

To determine whether endogenous RKIP binds endogenous importin α, MDA-MB-231 cells were plated onto 150-mm tissue culture–treated plates. The cells were lysed 72 h later with ice-cold 50 mM Tris–HCl (pH 7.4), 150 mM sodium

chloride, 5 mM EDTA, 1% Triton X-100, with protease inhibitor cocktail (Roche), and the extracts were clarified by centrifugation at 15,000*g* for 5 min at 4 °C. Total protein concentration was determined by Bradford assay (70). For coimmunoprecipitation, protein G beads were first incubated with 5 μg of mouse anti-RKIP/PEBP-1 antibody (Thermo Fisher; catalog no.: 37-2100) in 10 mM Tris–HCl (pH 7.4) for 1 h at 4 °C. The beads were pelleted by centrifugation at 2400*g* for 5 min at 4 °C (here and later between steps), blocked with 2% bovine serum albumin in 10 mM Tris–HCl (pH 7.4) for 30 min at 4 °C, then washed with 10 mM Tris-HCl (pH 7.4). Clarified cell lysates (200 μl at 4 mg/ml protein concentration) were added to the bead samples, with rotation for 2 h at 4 °C. The beads were washed twice with 10 mM Tris (pH 7.4), 150 mM NaCl, and 0.2% Triton X-100. Proteins were eluted from the beads with SDS sample buffer and then separated by SDS-PAGE. After membrane transfer, the blots were cut in half by molecular weight. The upper part was probed with rat anti-importin α5/α7 (karyopherin α1/α6) antibody (1:200 dilution; Santa Cruz Biotechnology, catalog no.: sc-101340), and the bottom part with the anti-RKIP antibody (1:5000 dilution) for 2 h at room temperature. The membranes were incubated with the appropriate goat anti-rat or goat anti-mouse IgG-horseradish peroxidase secondary antibody (Sigma-Aldrich), with proteins visualized by chemiluminescence.

Data availability

All data that support the findings of this study are available from the corresponding author upon request.

Acknowledgments—We thank Szilvia Pataki, Péter Germán, and Eric Cheng for technical assistance. This work was supported by the US National Institutes of Health grant GM07762, the Hungarian Thematic Excellence Progamme, the Hungarian Eötvös Loránd Research Network, the University of Toledo Foundation, Research Grant and Stimulus Funding from the College of Medicine and Life Sciences of the University of Toledo, the Dasman Diabetes Institute, and a gift from Clement Lam of Fully Honest Corp.

Author contributions—G. F. and K. C. Y. conceptualization; C. E. A., C. F., S. B., A. G., K. C. Y., and G. F. investigation; C. E. A., C. F., and G. F. formal analysis; G. F. writing–original draft; G. F. and K. C. Y. writing–review and editing; G. F. and K. C. Y. supervision; G. F. and K. C. Y. funding acquisition; G. F. project administration.

Conflict of interest—The authors declare that they have no conflicts of interest with the contents of this article.

Abbreviations—The abbreviations used are: ERK, extracellular signal-regulated kinase; GRK2, G protein-coupled receptor kinase 2; GST, glutathione-S-transferase; IgG, immunoglobulin G; IKK, inhibitor of κB kinase; MAPK, mitogen-activated protein kinase; MDCK, Madin-Darby canine kidney; NEBD, nuclear membrane breakdown; NLS, nuclear localization signal; PDB, Protein Data Bank; PEBP, phosphatidylethanolamine-binding protein; RFP, red fluorescent protein; RKIP, Raf kinase inhibitor protein.

References

1. Yesilkanal, A. E., and Rosner, M. R. (2014) Raf kinase inhibitory protein (RKIP) as a metastasis suppressor: regulation of signaling networks in cancer. *Crit. Rev. Oncog.* **19**, 447–454
2. Ling, H. H., Mendoza-Viveros, L., Mehta, N., and Cheng, H. Y. M. (2014) Raf kinase inhibitory protein (RKIP): functional pleiotropy in the mammalian brain. *Crit. Rev. Oncog.* **19**, 505–516
3. Lorenz, K., Schmid, E., and Deiss, K. (2014) Rkip: a governor of intracellular signaling. *Crit. Rev. Oncog.* **19**, 489–496
4. Rajkumar, K., Nichita, A., Anoor, P. K., Raju, S., Singh, S. S., and Burgula, S. (2016) Understanding perspectives of signalling mechanisms regulating PEBP1 function. *Cell Bioch. Funct.* **34**, 394–403
5. Lorenz, K., Rosner, M. R., Brand, T., and Schmitt, J. P. (2017) Raf kinase inhibitor protein: lessons of a better way for β-adrenergic receptor activation in the heart. *J. Physiol.* **595**, 4073–4087
6. Al-Mulla, F., Bitar, M. S., Taqi, Z., and Yeung, K. C. (2013) Rkip: much more than Raf kinase inhibitory protein. *J. Cell. Physiol.* **228**, 1688–1702
7. Datar, I., Tegegne, H., Qin, K., Al-Mulla, F., Bitar, M. S., Trumbly, R. J., *et al.* (2014) Genetic and epigenetic control of RKIP transcription. *Crit. Rev. Oncog.* **19**, 417–430
8. Yesilkanal, A. E., and Rosner, M. R. (2018) Targeting Raf kinase inhibitory protein regulation and function. *Cancers (Basel).* **10**, 306
9. Gabriela-Freitas, M., Pinheiro, J., Raquel-Cunha, A., Cardoso-Carneiro, D., and Martinho, O. (2019) RKIP as an inflammatory and immune system modulator: implications in cancer. *Biomolecules* **9**, 769
10. Moffit, J. S., Boekelheide, K., Sedivy, J. M., and Klysik, J. (2007) Mice lacking Raf kinase inhibitor protein-1 (RKIP-1) have altered sperm capacitation and reduced reproduction rates with a normal response to testicular injury. *J. Androl.* **28**, 883–890
11. Theroux, S., Pereira, M., Casten, K. S., Burwell, R. D., Yeung, K. C., Sedivy, J. M., *et al.* (2007) Raf kinase inhibitory protein knockout mice: expression in the brain and olfaction deficit. *Brain Res. Bull.* **71**, 559–567
12. Yeung, K., Seitz, T., Li, S., Janosch, P., McFerran, B., Kaiser, C., *et al.* (1999) Suppression of Raf-1 kinase activity and MAP kinase signalling by RKIP. *Nature* **401**, 173–177
13. Yeung, K., Janosch, P., McFerran, B., Rose, D. W., Mischak, H., Sedivy, J. M., *et al.* (2000) Mechanism of suppression of the Raf/MEK/extracellular signal-regulated kinase pathway by the Raf kinase inhibitor protein. *Mol. Cell. Biol.* **20**, 3079–3085
14. Corbit, K. C., Trakul, N., Eves, E. M., Diaz, B., Marshall, M., and Rosner, M. R. (2003) Activation of Raf-1 signaling by protein kinase C through a mechanism involving Raf kinase inhibitory protein. *J. Biol. Chem.* **278**, 13061–13068
15. Lorenz, K., Lohse, M. J., and Quitterer, U. (2003) Protein kinase C switches the Raf kinase inhibitor from Raf-1 to GRK-2. *Nature* **426**, 574–579
16. Park, S., Yeung, M. L., Beach, S., Shields, J. M., and Yeung, K. C. (2005) RKIP downregulates B-Raf kinase activity in melanoma cancer cells. *Oncogene* **24**, 3535–3540
17. Trakul, N., Menard, R. E., Schade, G. R., Qian, Z., and Rosner, M. R. (2005) Raf kinase inhibitory protein regulates Raf-1 but not B-Raf kinase activation. *J. Biol. Chem.* **280**, 24931–24940
18. Yeung, K. C., Rose, D. W., Dhillon, A. S., Yaros, D., Gustafsson, M., Chatterjee, D., *et al.* (2001) Raf kinase inhibitor protein interacts with NF-κB-inducing kinase and TAK1 and inhibits NF-κB activation. *Mol. Cell. Biol.* **21**, 7207–7217
19. Tang, H., Park, S., Sun, S. C., Trumbly, R., Ren, G., Tsung, E., *et al.* (2010) RKIP inhibits NF-κB in cancer cells by regulating upstream signaling components of the IκB kinase complex. *FEBS Lett.* **584**, 662–668
20. Bernier, I., Tresca, J. P., and Jolles, P. (1986) Ligand-binding studies with a 23 kDa protein purified from bovine brain cytosol. *Biochim. Biophys. Acta* **871**, 19–23
21. Banfield, M. J., Barker, J. J., Perry, A. C. F., and Brady, R. L. (1998) Function from structure? The crystal structure of human phosphatidylethanolamine-binding protein suggests a role in membrane signal transduction. *Structure* **6**, 1245–1254

22. Atmanene, C., Laux, A., Glattard, E., Muller, A., Schoentgen, F., Metz-Boutigue, M. H., *et al.* (2009) Characterization of human and bovine phosphatidylethanolamine-binding protein (PEBP/RKIP) interactions with morphine and morphine-glucuronides determined by noncovalent mass spectrometry. *Med. Sci. Monit.* **15**, BR178–B187
23. Al-Mulla, F., Hagan, S., Behbehani, A. I., Bitar, M. S., George, S. S., Going, J. J., *et al.* (2006) Raf kinase inhibitor protein expression in a survival analysis of colorectal cancer patients. *J. Clin. Oncol.* **24**, 5672–5679
24. Eves, E. M., Shapiro, P., Naik, K., Klein, U. R., Trakul, N., and Rosner, M. R. (2006) Raf kinase inhibitory protein regulates Aurora B kinase and the spindle checkpoint. *Mol. Cell.* **23**, 561–574
25. Eves, E. M., and Rosner, M. R. (2010) MAP kinase regulation of the mitotic spindle checkpoint. *Met. Mol. Biol.* **661**, 497–505
26. Al-Mulla, F., Bitar, M. S., Taqi, Z., Rath, O., and Kolch, W. (2011) RAF kinase inhibitory protein (RKIP) modulates cell cycle kinetics and motility. *Mol. Biosyst.* **7**, 928–941
27. Chatterjee, D., Bai, Y., Wang, Z., Beach, S., Mott, S., Roy, R., *et al.* (2004) RKIP sensitizes prostate and breast cancer cells to drug-induced apoptosis. *J. Biol. Chem.* **279**, 17515–17523
28. Ma, J., Li, F., Liu, L., Cui, D., Wu, X., Jiang, X., *et al.* (2009) Raf kinase inhibitor protein inhibits cell proliferation but promotes cell migration in rat hepatic stellate cells. *Liver Int.* **29**, 567–574
29. Mc Henry, K. T., Ankala, S. V., Ghosh, A. K., and Fenteany, G. (2002) A non-antibacterial oxazolidinone derivative that inhibits epithelial cell sheet migration. *ChemBioChem* **3**, 1105–1111
30. Zhu, S., McHenry, K. T., Lane, W. S., *et al.*Mc Henry, K. T., Lane, W. S., and Fenteany, G. (2005) A chemical inhibitor reveals the role of Raf kinase inhibitor protein in cell migration. *Chem. Biol.* **12**, 981–991
31. Lee, H. C., Tian, B., Sedivy, J. M., Wands, J. R., and Kim, M. (2006) Loss of Raf kinase inhibitor protein promotes cell proliferation and migration of human hepatoma cells. *Gastroenterology* **131**, 1208–1217
32. Mc Henry, K. T., Montesano, R., Zhu, S., Beshir, A. B., Tang, H. H., Yeung, K. C., *et al.* (2008) Raf kinase inhibitor protein positively regulates cell–substratum adhesion while negatively regulating cell–cell adhesion. *J. Cell. Biochem.* **103**, 972–985
33. Beshir, A. B., Ren, G., Magpusao, A. N., Barone, L. M., Yeung, K. C., and Fenteany, G. (2010) Raf kinase inhibitor protein suppresses nuclear factor-κB-dependent cancer cell invasion through negative regulation of matrix metalloproteinase expression. *Cancer Lett.* **299**, 137–149
34. Ojika, K., Katada, E., Tohdoh, N., Mitake, S., Otsuka, Y., Matsukawa, N., *et al.* (1995) Demonstration of deacetylated hippocampal cholinergic neurostimulating peptide and its precursor protein in rat tissues. *Brain Res.* **701**, 19–27
35. Tohdoh, N., Tojo, S., Agui, H., and Ojika, K. (1995) Sequence homology of rat and human HCNP precursor proteins, bovine phosphatidylethanolamine-binding protein and rat 23-kDa protein associated with the opioid-binding protein. *Brain Res. Mol. Brain Res.* **30**, 381–384
36. Okita, K., Matsukawa, N., Maki, M., Nakazawa, H., Katada, E., Hattori, M., *et al.* (2009) Analysis of DNA variations in promoter region of HCNP gene with Alzheimer's disease. *Biochem. Biophys. Res. Commun.* **379**, 272–276
37. Goumon, Y., Angelone, T., Schoentgen, F., Chasserot-Golaz, S., Almas, B., Fukami, M. M., *et al.* (2004) The hippocampal cholinergic neurostimulating peptide, the N-terminal fragment of the secreted phosphatidylethanolamine-binding protein, possesses a new biological activity on cardiac physiology. *J. Biol. Chem.* **279**, 13054–13064
38. Perry, A. C. F., Hall, L., Bell, A. E., and Jones, R. (1994) Sequence analysis of a mammalian phospholipid-binding protein from testis and epididymis and its distribution between spermatozoa and extracellular secretions. *Biochem. J.* **301**, 235–242
39. Cantwell, H., and Nurse, P. (2019) Unravelling nuclear size control. *Curr. Genet.* **65**, 1281–1285
40. Lu, J., Wu, T., Zhang, B., Liu, S., Song, W., Qiao, J., *et al.* (2021) Types of nuclear localization signals and mechanisms of protein import into the nucleus. *Cell Commun. Signal.* **19**, 1–10
41. Lange, A., Mills, R. E., Lange, C. J., Stewart, M., Devine, S. E., and Corbett, A. H. (2007) Classical nuclear localization signals: definition, function, and interaction with importin α. *J. Biol. Chem.* **282**, 5101–5105
42. Kosugi, S., Hasebe, M., Tomita, M., and Yanagawa, H. (2009) Systematic identification of cell cycle-dependent yeast nucleocytoplasmic shuttling proteins by prediction of composite motifs. *Proc. Natl. Acad. Sci. U. S. A.* **106**, 10171–10176
43. Oka, M., and Yoneda, Y. (2018) Importin α: functions as a nuclear transport factor and beyond. *Proc. Jpn. Acad. Ser. B, Phys. Biol. Sci.* **94**, 259–274
44. Wing, C. E., Fung, H. Y. J., and Chook, Y. M. (2022) Karyopherin-mediated nucleocytoplasmic transport. *Nat. Rev. Mol. Cell Biol.* **23**, 307–328
45. Görlich, D., Kostka, S., Kraft, R., Dingwall, C., Laskey, R. A., Hartmann, E., *et al.* (1995) Two different subunits of importin cooperate to recognize nuclear localization signals and bind them to the nuclear envelope. *Curr. Biol.* **5**, 383–392
46. Seedorf, M., Damelin, M., Kahana, J., Taura, T., and Silver, P. A. (1999) Interactions between a nuclear transporter and a subset of nuclqear pore complex proteins depend on Ran GTPase. *Mol. Cell. Biol.* **19**, 1547–1557
47. Nardozzi, J. D., Lott, K., and Cingolani, G. (2010) Phosphorylation meets nuclear import: a review. *Cell Commun. Signal.* **8**, 32
48. Fontes, M. R., Teh, T., Toth, G., John, A., Pavo, I., Jans, D. A., *et al.* (2003) Role of flanking sequences and phosphorylation in the recognition of the simian-virus-40 large T-antigen nuclear localization sequences by importin-α. *Biochem. J.* **375**, 339–349
49. Daniel, S., Bradley, G., Longshaw, V. M., Soti, C., Csermely, P., and Blatch, G. L. (2008) Nuclear translocation of the phosphoprotein Hop (Hsp70/Hsp90 organizing protein) occurs under heat shock, and its proposed nuclear localization signal is involved in Hsp90 binding. *Biochim. Biophys. Acta* **1783**, 1003–1014
50. Cokol, M., Nair, R., and Rost, B. (2000) Finding nuclear localization signals. *EMBO Rep.* **1**, 411–415
51. La Cour, T., Kiemer, L., Mølgaard, A., Gupta, R., Skriver, K., and Brunak, S. (2004) Analysis and prediction of leucine-rich nuclear export signals. *Protein Eng. Des. Sel.* **17**, 527–536
52. Xu, D., Marquis, K., Pei, J., Fu, S.-C., Cağatay, T., Grishin, N. V., *et al.* (2015) LocNES: A computational tool for locating classical NESs in CRM1 cargo proteins. *Bioinformatics* **31**, 1357–1365
53. Serre, L., Vallee, B., Bureaud, N., Schoentgen, F., and Zelwer, C. (1998) Crystal structure of the phosphatidylethanolamine-binding protein from bovine brain: a novel structural class of phospholipid-binding proteins. *Structure* **6**, 1255–1265
54. Simister, P. C., Burton, N. M., and Brady, R. L. (2011) Phosphotyrosine recognition by the Raf kinase inhibitor protein. *For. Immunopathol. Dis. Ther.* **2**, 59–70
55. Granovsky, A. E., Clark, M. C., McElheny, D., Heil, G., Hong, J., Liu, X., *et al.* (2009) Raf kinase inhibitory protein function is regulated *via* a flexible pocket and novel phosphorylation-dependent mechanism. *Mol. Cell Biol.* **29**, 1306–1320
56. Simister, P. C., Banfield, M. J., and Brady, R. L. (2002) The crystal structure of PEBP-2, a homologue of the PEBP/RKIP family. *Acta Crystallogr. D Biol. Crystallogr.* **58**, 1077–1080
57. Seibel, N. M., Eljouni, J., Nalaskowski, M. M., and Hampe, W. (2007) Nuclear localization of enhanced green fluorescent protein homomultimers. *Anal. Biochem.* **368**, 95–99
58. Li, C., Goryaynov, A., and Yang, W. (2016) The selective permeability barrier in the nuclear pore complex. *Nucleus* **7**, 430–446
59. Michaelson, D., Silletti, J., Murphy, G., D'Eustachio, P., Rush, M., and Philips, M. R. (2001) Differential localization of Rho GTPases in live cells: regulation by hypervariable regions and RhoGDI binding. *J. Cell Biol.* **152**, 111–126
60. Lanning, C. C., Ruiz-Velasco, R., and Williams, C. L. (2003) Novel mechanism of the co-regulation of nuclear transport of SmgGDS and Rac1. *J. Biol. Chem.* **278**, 12495–12506
61. Michaelson, D., Abidi, W., Guardavaccaro, D., Zhou, M., Ahearn, I., Pagano, M., *et al.* (2008) Rac1 accumulates in the nucleus during the G2

phase of the cell cycle and promotes cell division. *J. Cell. Biol.* **181**, 485–496
62. Schwamborn, K., Albig, W., and Doenecke, D. (1998) The histone H1° contains multiple sequence elements for nuclear targeting. *Exp. Cell Res.* **244**, 206–217
63. Nakahara, S., Hogan, V., Inohara, H., and Raz, A. (2006) Importin-mediated nuclear translocation of galectin-3. *J. Biol. Chem.* **281**, 39649–39659
64. Nakahara, S., Oka, N., Wang, Y., Hogan, V., Inohara, H., and Raz, A. (2006) Characterization of the nuclear import pathways of galectin-3. *Cancer Res.* **66**, 9995–10006
65. Her, L. S., Lund, E., and Dahlberg, J. E. (1997) Inhibition of Ran guanosine triphosphatase-dependent nuclear transport by the matrix protein of vesicular stomatitis virus. *Science* **276**, 1845–1848
66. Von Kobbe, C., Van Deursen, J. M. A., Rodrigues, J. P., Sitterlin, D., Bachi, A., Wu, X., *et al*. (2000) Vesicular stomatitis virus matrix protein inhibits host cell gene expression by targeting the nucleoporin Nup98. *Mol. Cell.* **6**, 1243–1252
67. Petersen, J. M., Her, L.-S., Varvel, V., Lund, E., and Dahlberg, J. E. (2000) The matrix protein of vesicular stomatitis virus inhibits nucleocytoplasmic transport when it is in the nucleus and associated with nuclear pore complexes. *Mol. Cell. Biol.* **20**, 8590–8601
68. Glodowski, D. R., Petersen, J. M., and Dahlberg, J. E. (2002) Complex nuclear localization signals in the matrix protein of vesicular stomatitis virus. *J. Biol. Chem.* **277**, 46864–46870
69. Ran, F. A., Hsu, P. D., Wright, J., Agarwala, V., Scott, D. A., and Zhang, F. (2013) Genome engineering using the CRISPR-Cas9 system. *Nat. Protoc.* **8**, 2281–2308
70. Bradford, M. M. (1976) A rapid and sensitive method for the quantitation of microgram quantities of protein utilizing the principle of protein-dye binding. *Anal. Biochem.* **72**, 248–254